Progress In Electromagnetics Research, Vol. 139, 445–478, 2013

EXPOSURE OPTIMIZATION IN INDOOR WIRELESS NETWORKS BY HEURISTIC NETWORK PLANNING

David Plets*, Wout Joseph, Kris Vanhecke, and Luc Martens

Department of Information Technology, WiCa-Ghent University/iMinds, Gaston Crommenlaan 8, B-9050 Ghent, Belgium

Abstract—Due to the increased use of indoor wireless networks and the concern about human exposure to radio-frequency sources, exposure awareness has increased during recent years. However, current-day network planners rarely take into account electric-field strengths when designing networks. Therefore, in this paper, a heuristic indoor network planner for exposure calculation and optimization of wireless networks is developed, jointly optimizing coverage and exposure, for homogeneous or heterogeneous networks. The implemented exposure models are validated by simulations and measurements. As a first novel optimization feature, networks are designed that do not exceed a user-defined electric-field strength value in the building. The influence of the maximally allowed field strength, based on norms in different countries, and the assumed minimal separation between the access point and the human are investigated for a typical office building. As a second feature, a novel heuristic exposure minimization algorithm is presented and applied to a wireless homogeneous WiFi and a heterogeneous WiFi-LTE femtocell network, using a new metric that is simple but accurate. Field strength reductions of a factor 3 to 6 compared to traditional network deployments are achieved and a more homogeneous distribution of the observed field values on the building floor is obtained. Also, the influence of the throughput requirement on the field strength distribution on the building floor is assessed. Moreover, it is shown that exposure minimization is more effective for high than for low throughput requirements and that high field values are more reduced than low field values.

Received 30 January 2013, Accepted 26 March 2013, Scheduled 5 May 2013
* Corresponding author: David Plets (david.plets@intec.ugent.be).

1. INTRODUCTION

Due to the increased popularity of indoor wireless networks, many software tools have been developed for the prediction of the received signal quality and the network performance [1–7]. These tools are either based on ray models, numerical solver models, heuristic predictions, or statistical (site-specific) models. In [8], the authors developed a heuristic indoor propagation prediction tool, which is able to design and optimize a WiFi network for a given coverage requirement with a minimal number of access points (APs).

In the meanwhile, both the trend towards green networking [9, 10] as well as the enormous increase of wireless communication due to the increasing need for coverage and high data rates, make it necessary to investigate and characterize the exposure of the general public to electromagnetic fields at RF (radio-frequency) frequencies used for wireless telecommunication. Measurements and studies have indicated that indoor exposure cannot be neglected [11]. International safety guidelines such as [12] and ICNIRP (International Commission on Non-Ionizing Radiation Protection) [13] have been developed and authorities and countries have implemented laws and norms to limit human exposure. This indicates the need for an accurate exposure characterization and exposure-aware network planning. Consequently, research has recently been started on *green* network deployments. Besides attempts to limit energy consumption in wireless (access) networks [10, 14], the concerns about a possible harmful impact of human exposure to RF sources have led to a situation where network planners (out of necessity) have to take the field strength of the incident waves into account.

However, most research still focuses on the mere *characterization* of RF exposure in different environments and/or for different technologies [15–19], or for MIMO [20] networks and terminals, without focusing on an actual reduction or minimization of the exposure. Other studies try to predict or simulate the 'impact' of a deployment. E.g., in [21], a metric is proposed to assess the environmental impact of network deployments. The metric focuses on outdoor environments and after some preprocessing of different configurations, the impact of a particular deployment can be assessed. In the study, however, no (automatic) network planning is performed and configurations are assessed based on their environmental impact, not on their coverage. In [22], base-station networks are optimized based on a metric which not only takes into account coverage, traffic, and economic efficiency, but also the environmental impact of the electromagnetic field. The optimization is based on a genetic algorithm, just like in [23], where

automatic green (i.e., low energy consumption, low carbon emissions, low exposure) network planning is performed. Both papers, however, are aimed at outdoor environments, often for which simple propagation models are used, permitting the usage of genetic algorithms, due to the short calculation time of a single iteration.

In this paper, an advanced exposure calculation model and two *automatic indoor exposure optimization algorithms* for network planning are presented that jointly optimize exposure and coverage. The model for the electric-field strength distribution is constructed and validated with simulations and measurements for a WiFi access point and an Long-Term Evolution (LTE) femtocell. The paper describes two optimization algorithms, both of which are very useful in everyday network planning. Firstly, an exposure limitation algorithm is described. It designs a network that provides a user-defined coverage with the lowest possible amount of access points, while at the same ensuring that a user-defined exposure threshold is not exceeded at any location on the entire building floor. The influence on the network layout of the maximally allowed field strength and of the assumed minimal separation between the AP and the human are assessed for a typical office building and for exposure limits (or recommendations) in different regions in the world. To the authors' knowledge, similar algorithms have not been presented yet. Secondly, an exposure minimization algorithm is described, which designs a network which provides a user-defined coverage, with the lowest possible resulting exposure (within reasonable transmit power restrictions). Exposure is minimized in an office building for a homogeneous WiFi (Wireless Fidelity) network and, in the light of the emergence of new wireless technologies such as LTE [11, 19], also for a heterogeneous WiFi-LTE network. A homogeneous network is a single-technology network, i.e., only transmitters of one single technology are present (e.g., WiFi access points). Heterogeneous networks on the contrary, are cooperative networks allowing receivers to connect to and perform handovers between transmitters from different technologies, e.g., a 4G phone connecting to WiFi access points or LTE femtocells. Exposure distributions are compared for an exposure-optimized network design and a traditional network design (with maximal-power indoor transmitters), and for different throughputs in the building. Also, the exposure reduction after optimization is determined. Due to the heuristic approach, the algorithm is much faster than classical genetic algorithms, which require a lot of 'unintelligent' iterations before converging to an acceptable solution.

The use of femtocells for exposure reduction has already been

investigated in [19]. The influence of using an Universal Mobile Telecommunications System (UMTS) femtocell on the received and transmitted power levels of a mobile device is assessed, but no actual network optimization is performed. Until now, indoor network planning rarely took into account, let alone optimized exposure. This paper is one of the first to describe and apply automatic planning algorithms for exposure-optimized indoor networks, using an advanced prediction model that has been extensively validated by actual measurements. Moreover, this paper does not only investigate homogeneous wireless networks, but also the emerging heterogeneous networks, for which exposure minimization has not been investigated yet.

In Section 2 the network planner and its configuration is presented and a definition of homogeneous and heterogeneous networks is provided. In Section 3, the exposure model is constructed and validated. Section 4 discusses the exposure algorithm, followed by an analysis of the application of exposure limitation algorithm in Section 5 and the exposure minimization algorithm in Section 6. Section 7 investigates the validity of the assumption that the field strength is mainly determined by the dominant transmitter and in Section 8, the conclusions of this research are presented.

2. NETWORK PLANNER AND DEFINITIONS

2.1. Network Planner

The WiCa Heuristic Indoor Propagation Prediction (WHIPP) algorithm is heuristic planning algorithm, developed and validated for the prediction of path loss in indoor environments [8]. It takes into account the effect of the environment on the wireless propagation channel and has been developed for the prediction of the path loss on a grid over an entire building floor or at specific locations. The granularity of the prediction is determined by the density of the grid points on the building floor. The algorithm bases its calculations on the determination of the dominant path between transmitter and receiver, i.e., the path along which the signal encounters the lowest obstruction. This approach is justified by the fact that more than 95% of the energy received is contained in only 2 or 3 paths [3]. The dominant path is determined with a multidimensional optimization algorithm that searches the lowest total path loss, consisting of a distance loss (taking into account the length of the propagation path), a cumulated wall loss (taking into account the walls penetrated along the propagation path), and an interaction loss (taking into account the propagation direction changes of the path, e.g., around corners). The model has

been constructed for the 2.4–2.6 GHz band and its performance has been validated with a large set of measurements in various buildings [8]. In contrary to many existing tools no tuning of the tool's parameters is performed for the validation. Excellent correspondence between measurements and predictions is obtained, even for other buildings and floors [8]. As the distance loss contribution in the tool is based on the free-space loss model for every environment, the tool is generally applicable, while other tools are often too dependent of the environment upon which the used propagation model is based.

2.1.1. Network Planner Settings

In the following, we will list the network planner settings that will be used for the design of exposure-optimized networks.

Two receivers will be considered: a WiFi receiver (e.g., a laptop with a WiFi receiver chipset) and an LTE receiver (e.g., a 4G mobile phone). Table 1 lists the assumed receiver sensitivities of the WiFi chipset (2.4 GHz band), a reference receiver for 802.11 g. The table shows the required received power P_{Rx} [dBm] in order to achieve a certain physical-layer (PHY) throughput. The assumed receiver antenna gain is 0 dB. For the LTE receiver chipset (2.6 GHz band), a bandwidth of 20 MHz, a DL : UL (downlink : uplink) ratio of 3 : 1 (i.e., three quarters of the available bandwidth is available for downstream traffic), a noise figure of 8 dB, and SNR (signal-to-noise-ratio) values from [24] are assumed, yielding the receiver sensitivities listed in Table 1, column 'LTE'.

For the actual network planning calculations, the 90% shadowing margin, the 95% fade margin, and the interference margin are chosen as 7 dB, 5 dB, and 0 dB, respectively [8]. The prediction model presented in [8] is developed for 2.4 and 2.6 GHz. Wall penetration losses and interaction losses [8] are assumed to be the same due to the small frequency difference (2.6 GHz vs. 2.4 GHz), but the distance loss is adapted by taking into account the frequency dependence of the distance loss model [8].

2.2. Definition of Homogeneous and Heterogeneous Networks

In this paper, planning for exposure-optimized networks will be performed for both a homogeneous WiFi network and a heterogeneous WiFi-LTE network.

A *homogeneous* network is a single-technology network, i.e., the considered network only consists of transmitters of one single technology. For the homogeneous scenarios considered here, we will

Table 1. Sensitivities of the WiFi and LTE receivers (20 MHz channel) and margin settings used in the network planner.

Receiver sensitivities			
WiFi 802.11 g		**LTE (20 MHz channel)**	
$\mathbf{P_{Rx}}$ **[dBm]**	**PHY throughput [Mbps]**	$\mathbf{P_{Rx}}$ **[dBm]**	**PHY throughput [Mbps]**
−88	6	−92.6	8.5
−87	9	−88.1	12.7
−84	12	−80.6	16.9
−82	18	−77.1	25.3
−79	24	−72.1	33.8
−75	36	−68.1	40.6
−68	48	−61.7	50.7
−68	54		
Margin settings			
Shadowing margin		7 dB	
Fade margin		5 dB	
Interference margin		0 dB	

also assume that there are no transmitters using other technologies present in the building. The homogeneous network we will investigate is a network with only 2.4 GHz WiFi access points, in which a WiFi receiver is located (e.g., a laptop or a mobile phone). Although a background field level will be present due to other technologies (e.g., FM (Frequency Modulation) radio), this will not influence the actual optimization later in this paper. If the field level is known though, it can easily be taken into account in the actual exposure characterization within the building.

A *heterogeneous* network is a cooperative network formed by a collaboration of networks that use different technologies. It allows receivers to connect to and perform handovers between transmitters from different technologies. Here, a heterogeneous network with 2.4 GHz WiFi access points and 2.6 GHz LTE femtocells will be investigated. As receiver device, we use a 4G mobile phone with both a WiFi and an LTE receiver chipset, allowing it to connect to both transmitters types. The same WiFi receiver chipset as for the homogenenous network is assumed (see Table 1, column 'WiFi'). The LTE receiver chipset is described in Section 2.1.1 and Table 1, column

'LTE'. In the remainder of the paper, we will again only take into account the fields caused by the WiFi and LTE transmitters.

3. EXPOSURE MODEL

3.1. Construction of the Exposure Model

In this section, the model to predict the electric-field strength caused by a transmitter will be derived. In [25], a far-field conversion formula between path loss and electric-field strength is presented.

$$\text{PL [dB]} = 139 - E_{\text{ERP=1 kW}}\ [\text{dB}\mu\text{V/m}] + 20 \cdot \log_{10}(f)\ [\text{MHz}], \quad (1)$$

with PL [dB] the path loss between the transmitter and a receiver at a certain location, $E_{\text{ERP=1 kW}}$ [dBμV/m] the received field strength for an ERP (Effective Radiated Power) of 1 kW, and f [MHz] the frequency.

Using Equation (1) and the identity

$$E\ [\text{V/m}] = E_{\text{ERP=1 kW}}\ [\text{V/m}] \cdot \sqrt{\text{ERP [kW]}}, \quad (2)$$

and knowing that for dipoles ERP [dBm] = EIRP [dBm] − 2.15, we obtain the following formula for the electric-field strength E [V/m] at a certain location, as a function of the EIRP, the path loss, and the frequency:

$$E\ [\text{V/m}] = 10^{\frac{\text{EIRP [dBm]} - 43.15 + 20 \cdot \log_{10}(f)\ [\text{MHz}] - \text{PL [dB]}}{20}}, \quad (3)$$

For the path loss PL of Equation (3), the extensively validated WHIPP model of [8] is used (see also Section 2.1). The assumed duty cycle is 100% (worst-case scenario).

3.2. Validation of the Exposure Model

The electric-field model of Equation (3), with the PL calculated according to the WHIPP model, has also been validated in the proximity of a WiFi access point and an LTE femtocell, with simulations and measurements.

For the validation *simulations* at the two frequencies (2.4 and 2.6 GHz), the antenna of the access point is modeled as a half-wavelength dipole. The maximum grid step does not exceed 0.07 times the wavelength in free space. Using FDTD (Finite-Difference Time-Domain) calculations, the simulation domain is finite in extent and boundary conditions are applied. Uni-axial perfectly matched layers (UPML) are applied to the boundaries to avoid reflections back into the simulation domain. The number of layers is automatically set by

the FDTD solver to obtain a selected efficiency of 99.9%. Electric-field strength simulations are executed for a dipole EIRP (Equivalent Isotropically Radiated Power) of 20 dBm and at distances between 3.5 and 50 cm from the dipole.

The validation *measurements* for a WiFi DLink access point have been performed using the methodology described in [26]. Firstly, the active WLAN channels are determined by means of a WLAN-packet analyzer. Secondly, the duty cycle of these active channels is determined, and thirdly, max-hold measurements of the electric-field of the different WLAN channels are executed with a spectrum analyzer and a calibrated tri-axial measurement probe. Finally, the total average electric field is calculated by multiplying the square root of the appropriate duty cycle with the recorded max-hold value. The measurements are executed in the vicinity of a WiFi DLink DI-624 AirPlusXtremeG AP with an EIRP of 20 dBm and a duty cycle of 100%.

Figure 1(a) compares the simulated (half-wavelength dipole at 2400 MHz) and measured electric-field strength with the field strengths prediction by the WHIPP model (see Equation (3)), as a function of the separation d from the dipole. The figure shows that the electric-field strength as predicted by the WHIPP model is a very good approximation for both the *measured* and *simulated* near-

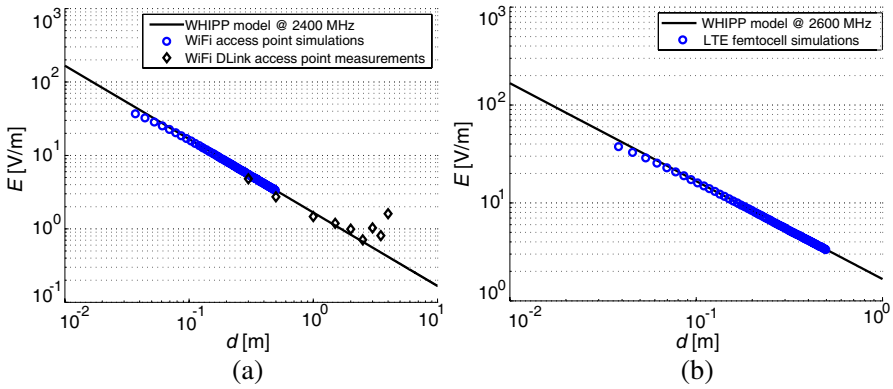

Figure 1. (a) Measured electric-field strength in the vicinity of a DLink DI-624 AP with an EIRP of 20 dBm, electric-field strength in the vicinity of a dipole at 2400 MHz with an EIRP of 20 dBm according to FDTD simulations, and WHIPP model prediction. (b) Electric-field strength in the vicinity of a dipole at 2600 MHz with an EIRP of 2 dBm according to FDTD simulations, and WHIPP model prediction.

field electric-field strength. Average deviations of 0.07 V/m (with a standard deviation of 0.08 V/m) are obtained for the WiFi access point simulations for distances larger than 10 cm. The measurements deviate from the model 0.08 V/m on average (0.43 V/m in absolute deviations) with a standard deviation of 0.58 V/m. The higher measured deviations at larger separations may be due to wall reflections.

Figure 1(b) compares the simulated (half-wavelength dipole at 2600 MHz) with the field strengths prediction by the WHIPP model (see Equation (3)), as a function of the separation d from the dipole. The figure shows that again, the electric-field strength as predicted by the WHIPP model is a very good approximation for the simulated near-field electric-field strength. Average deviations of 0.06 V/m (with a standard deviation of 0.06 V/m) are obtained for distances larger than 10 cm.

3.3. Exposure Calculation for Multiple Sources

The previous model is directly applicable for networks with one transmitting source. However, in most cases, wireless networks consist of multiple transmitting sources and exposure calculation should take into account the fields from all sources. To calculate the electric-field strength at a certain location, we will only consider the electric-field strength E_{dom} caused by the most dominant source (i.e., the source causing the highest electric-field value at that location), in order to speed up the calculations. However, in Section 7, we will also investigate the impact of this simplification by comparing with an expression E_{total} that takes into account all contributing sources at a certain location.

$$E_{\text{total}} = \sqrt{\sum_{i=1}^{N} E_i^2}, \tag{4}$$

where N is the total number of different sources on the building floor. E_i is the electric-field strength caused by transmitting source i. The field vectors caused by the different sources are thus assumed to have no phase correlation.

4. EXPOSURE OPTIMIZATION ALGORITHMS

In this section, the *exposure limitation* algorithm and the *exposure minimization* algorithm will be presented. The exposure limitation algorithm creates a network that provides a certain requested coverage with a minimal number access points, while ensuring that a self-chosen

electric-field strength limit (e.g., 3 V/m) will nowhere be exceeded in the whole building, provided you keep a certain (self-chosen) distance from the transmitter (e.g., 50 cm). The exposure minimization algorithm will also provide the requested coverage in the building, but in such a way that the electric-field strength *over the entire building floor* is minimized. The aim of the algorithm is to minimize a metric that reflects 'the degree of human exposure' to RF sources on the entire building floor. The metric will be described in Section 4.2.1. For the calculation of the cumulative distribution function (cdf) of all electric-field strengths throughout the building, we will exclude the locations that are within 30 cm from the transmitters, because we can assume that people will not remain within a 30-cm range of the transmitter.

4.1. Exposure Limitation Algorithm

In this section, we will design a network that provides a certain required throughput in the different rooms of the building, but where the electric-field strength at a given minimal distance from the transmitter remains below a given threshold.

Figure 2 shows a flow graph summarizing the exposure limitation algorithm. There are three inputs for the algorithm: the assumed minimal separation d_s [m] of the human from the transmitters that will be installed, the maximally allowed electric-field strength $E_{ds}^{\max}$ [V/m] at a separation equal to d_s from the transmitter, and the ground plan of the building floor that is to be covered, with indication of the coverage requirement for each of the rooms. After using the WHIPP path loss calculator to determine the path loss PL_{ds} [dB] at a distance equal to d_s, and combining Eqs. (1) and (2), an expression for the corresponding maximally allowed ERP $\mathrm{ERP}_{\max}$ [kW] of the transmitters is obtained:

$$\mathrm{ERP}_{\max}\ [\mathrm{kW}] = (E_{ds}^{\max})^2\ [\mathrm{V/m}] \cdot 10^{\frac{\mathrm{PL}_{ds}\ [\mathrm{dB}] - 19 - 20\cdot\log_{10}(f)\ [\mathrm{MHz}]}{10}}. \quad (5)$$

After some simplifications, and given that for dipoles ERP [dBm] = EIRP [dBm] − 2.15, we obtain the following formula for the maximally allowed $\mathrm{EIRP}_{\max}$ [dBm]:

$$\mathrm{EIRP}_{\max}\ [\mathrm{dBm}] = 43.15 + 20 \cdot \log_{10}\left(\frac{E_{ds}^{\max}\ [\mathrm{V/m}]}{f\ [\mathrm{MHz}]}\right) + \mathrm{PL}_{ds}\ [\mathrm{dB}], \quad (6)$$

where $\mathrm{EIRP}_{\max}$ is limited to 20 dBm, the maximally allowed transmit power for WiFi in Europe in the 2.4 GHz band [27]. For the exposure calculations later in this paper, it will be assumed that this limit also applies to non-European countries. Fig. 1 shows that the WHIPP model is a good choice for the parameter PL_{ds} at small transmitter-receiver separations. After determining $\mathrm{EIRP}_{\max}$,

the WHIPP optimization module [8] delivers the ground plan with the transmitter locations (see Fig. 2).

Many countries have different limitations or guidelines for electric-field strengths: e.g., 6 V/m in Italy, 12 V/m in China, ... (for frequencies between 30 and 3000 MHz). Eq. (6) allows quickly determining the transmit power limit to meet these restrictions. Once $\mathrm{EIRP}_{\max}$ is known, the network planning algorithm described in [8] is used to design a network which satisfies both coverage and exposure requirements. The methodology creates a network that meets the different coverage requirements in the rooms on the building and where the observed electric-field strength E does not exceed the threshold value $E_{ds}^{\max}$ that was set by the user, in any of the locations on the building floor. The building floor is covered with the least number of access points possible, by maximizing the AP power within the imposed exposure limitations.

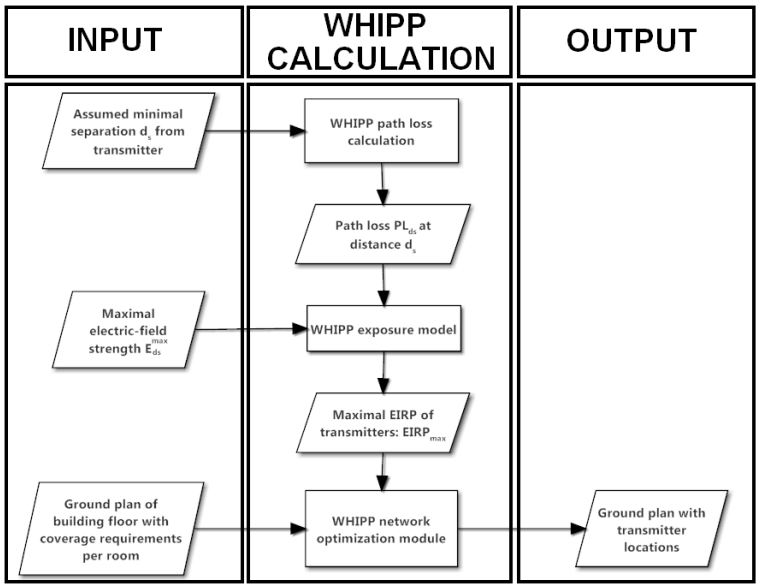

Figure 2. Flow graph of exposure limitation algorithm.

4.2. Exposure Minimization Algorithm

In this section, we will again design a network that provides a certain required throughput in the different rooms of the building, but where the *global exposure* will at the same time be minimal. To assess the

global exposure, an optimization metric reflecting the degree of human exposure on the building floor is needed.

4.2.1. Optimization Metric

There exist different metrics to assess, limit, or minimize the exposure on a building floor, e.g., [21, 23]. In this paper, we will use E_M, the average of the median electric-field strength E_{50} in the entire building, and the 95%-percentile value E_{95} of the field strengths in the building.

$$E_M = \frac{w_1 \cdot E_{50} + w_2 \cdot E_{95}}{w_1 + w_2} \left\{ \begin{array}{l} \text{with user-defined coverage} \\ \text{requirement for each location} \\ \text{according to 90\% shadowing} \\ \text{margin and 95\% fading margin} \end{array} \right. \quad (7)$$

with w_1 and w_2 weighting factors for the 50%-percentile value E_{50} and the 95%-percentile E_{95} respectively. We choose to include E_{50} into the metric to account for the median exposure on the building floor, and also E_{95}, to account for the maximal exposure values. Here, we will assume an equal impact of E_{50} and E_{95} on the metric and set both w_1 and w_2 at a value of 0.5. When evaluating and optimizing the different networks for a low exposure, the given coverage requirement always has to be met, using the 90% shadowing margin and 95% fading margin. The WHIPP tool allows choosing a separate coverage requirement for each room [8].

In the future, more complex metrics can be investigated. Each location on the building floor could be attributed a weight that corresponds to the likeliness that people are present at that location (number of people per m^2 per hour). This way, high field values could be avoided in rooms where people are likely to be present for a longer time.

Other metrics have been proposed in literature. In [21], an Electromagnetic Environmental Impact Factor (EEIF) has been defined, a scale from 0 to 100 to characterize the electromagnetic pollution level in an outdoor urban area. However, this approach is not applied to indoor environments and does not take into account coverage requirements. Moreover, it requires the definition of the best-case and worst-case reference scenarios corresponding with 0 and with 100 on the scale respectively. The EEIF takes into account the average electric-field value and the variance of the values. This is also the case for our metric, which gives preference to configurations with a low median field strength (use of E_{50}) and a low variance (use of E_{95}). In the metric of [23], only the median field strength over the investigated area is considered, which does not penalize high field strength fluctuations. In [22], a (green) optimization metric is used,

but it is aimed at (outdoor) cellular base station networks: besides coverage and electromagnetic field strength, also traffic aspects and economic efficiency are taken into account.

4.2.2. Algorithm

In this section, an algorithm is presented to minimize the *global* exposure metric E_M (average of median and 95%-percentile electric-field value, see Section 4.2.1) on a building floor. Lower values of E_M will lead to a larger number of access points, but with lower transmit power. The exposure minimization algorithm consists of four phases, displayed in the flow graph of Fig. 3.

(1) In the first phase, a network containing low-power access points with an EIRP of 1 dBm, is created. This is done according to the optimization algorithm presented in [8, 28]. This yields a network that covers the building floor according to the user's throughput requirements and with the given AP transmit power of 1 dBm (see Fig. 3). This low transmit power (1 dBm) is chosen because a network with many low-power transmitters is preferred over a network with few high-power transmitters (that still provides the same coverage though), due to the better exposure characteristics of the former network.

(2) In a second phase, it is investigated if access points within 125% of their line-of-sight range (circle around access point) from each other, can be merged into one new access point (with a possibly higher transmit power), yielding a new network with a lower E_M value. Practical experience has learned that the value of 125% is high enough to not exclude possibly mergeable access points, but not too high to needlessly investigate all access pairs. The merging of two access points is only executed if the value for the *global exposure* metric E_M is lower for the new network. Merging of an access point pair consists of removing the two access points of the pair and adding one new access point at an optimal location (= with a minimal EIRP). The access point pairs with the lowest separation between each other are first investigated, because they have the greatest probability of being merged. When merging, the optimal location of the new access point is chosen as follows. After removing the access point pair, it is calculated which receiver points do not receive a sufficient power from the remaining access points anymore: these receiver points will not obtain the requested coverage anymore and they are collected in a set L. We now want to cover all these points by placing a new transmitter with a transmit power that is as low as possible (for the purpose of a

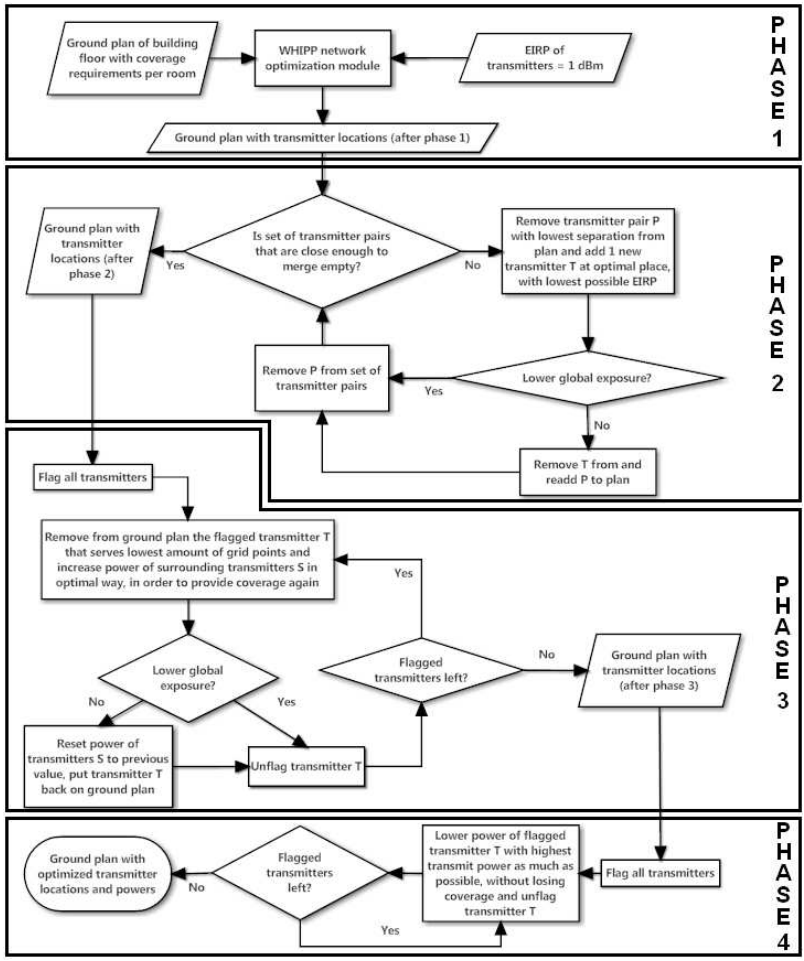

Figure 3. Flow graph of exposure minimization algorithm with indication of the four optimization phases.

low exposure). To find the location (*optimal merge location*) for this access point with a minimal power, we execute the following process, consisting of roughly three steps. Firstly, for each possible access point location, the algorithm first determines all path losses between that location and the locations of the other receiver points of L. Secondly, the maximum value of these path losses is stored for each possible access point location. Thirdly, the access point (location) that has the *lowest* stored maximum path loss value will now be able to cover L with the lowest possible power, and hence,

also the lowest exposure. Phase 2 is illustrated in Fig. 3, without going into detail on the three steps of the process of selecting the optimal merge location.

(3) In a third phase, it is checked if an access point can be removed by increasing the transmit powers of surrounding access points. The access points serving the least amount of grid points are first investigated, because these have the largest chance to be 'redundant' when small power increases are applied to the surrounding access points. The procedure of increasing the transmit powers of surrounding access points in an optimal way consists of roughly three steps and is executed as follows. Firstly, the grid points that lose coverage by removing the access point are determined. A grid point loses coverage if its received power becomes too low to provide the required throughput in that room. After removal of the access point, each of these grid points will thus have a 'received-power deficit' of a few dB, i.e., the best serving remaining transmitter will provide the grid point with a received power that is a few dB too low to obtain the required coverage. Secondly, the maximum value of the deficits over all grid points without coverage determines the necessary power increase of a first access point in the vicinity of the grid points that have lost coverage. After increasing the power of this access point, the size of the set of grid points that have lost coverage will decrease, thanks to some grid points 'regaining' coverage. It is assumed that a receiver always connects to the one access point that provides it with the highest received power. Thirdly, as long as this set is not empty, the transmit power of *other* surrounding access points is increased. Due to the nature of the algorithm, the consecutive power increases will decrease. An access point of which the power has already been increased, is excluded from further power increase operations, because for a low exposure, it is better to have a homogeneous distribution of (low) transmit powers than to have several high and several low transmit powers. This way, the coverage gaps are filled with the lowest possible exposure increase. Phase 3 is illustrated in Fig. 3, without going into detail on the three steps of the (optimal) way of selecting the access points for which the power is increased.

(4) In the fourth phase (see Fig. 3), it is investigated if the transmit power of the individual access points can be lowered without losing coverage. Access points with the highest transmit power are first investigated, because with respect to the global exposure value, it is more advantageous to lower these first. The algorithm allows setting a lower limit for the transmit power (e.g., 1 dBm) to satisfy

the access point configuration settings that are possible.

The resulting network is a network that provides the requested coverage with the lowest human exposure.

5. APPLICATION OF EXPOSURE LIMITATION ALGORITHM

In this section, the exposure limitation algorithm described in Section 4.1 will be applied to an actual building. Also, the influence of the imposed exposure restrictions on the network layout will be assessed.

5.1. Configuration

When evaluating and optimizing wireless networks for a low exposure, a given coverage requirement always has to be met. Fig. 4 shows the ground plan of the third floor (90 m × 17 m) of an office building in Ghent, Belgium, for which we will intend to limit the human exposure. The shaded rooms indicate the rooms and locations where no coverage is required; these are kitchens, toilets, storerooms, elevator shafts, ... In the other rooms, the user can define a certain required throughput (e.g., 54 Mbps, 18 Mbps, ...), which will be achieved during 95% of the time and at 90% of the locations, according to the margins defined in Table 1. For this specific case, the coverage requirement in the building will be 'HD video' streaming access (54 Mbps) throughout the entire building, except in the shaded rooms (see Section 4.2.1). Furthermore, only WiFi access points will be placed to form a homogeneous network. They are placed at a height of 200 cm

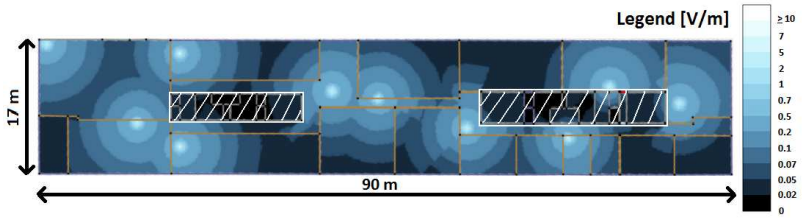

Figure 4. Ground plan of the building that is optimized for a maximal electric field of 5 V/m at a separation of 10 cm from the AP and indication of electric-field strength. The APs are located at the center of the lighter zones. The shaded area indicates where no wireless coverage is required.

above ground level and the receiver is assumed at a height of 100 cm above ground level.

5.2. Exposure Limitation for a Homogeneous WiFi Network for Different Exposure Restrictions

In this section, the influence of the exposure restrictions (assumed minimal separation d_s and maximal field-strength $E_{\max}^{ds}$ at a separation d_s) on the number of access points needed to cover the building floor is investigated. Fig. 5 shows the number of APs needed to provide the required coverage on the building floor, as a function of the maximal limit $E_{ds}^{\max}$ for different minimal separations d_s from the AP, ranging from 10 cm to 3 m. Also, the field exposure limits of some countries are indicated. These limits are listed in Table 2.

Table 2. Number of APs needed to cover the building floor depicted in Fig. 4, for exposure limits in different countries.

Number of required access points		**Separation d_s between Rx and AP [cm]**				
Region	**Limit [V/m]**	**10**	**30**	**50**	**100**	**300**
Salzburg	**0.02**	> 75	> 75	> 75	> 75	> 75
Wallonia[1]	**3**	16	5	4	3	3
Flanders[1]	**4.48**	11	4	3	3	3
Italy	**6**	6	3	3	3	3
China	**12**	4	3	3	3	3
(ICNIRP [29])	**61**	3	3	3	3	3

[1]: Wallonia and flanders are regions in Belgium.

Figure 5 shows that when, at a fixed separation from the AP, the maximally allowed exposure limit $E_{\max}^{ds}$ increases, a higher EIRP is allowed for the APs, leading to a lower total number of APs needed to cover the building floor. E.g., for a separation of 10 cm, a network with 16 access points is required according to the limit of 3 V/m in the Belgian region of Wallonia, while 4 access points suffice according to the Chinese limit of 12 V/m. At high field strength limits $E_{\max}^{ds}$, the number of APs becomes constant (3 access points required for $E_{\max}^{ds}$ values of 17 V/m or higher for all investigated separations), since the EIRP at 2.4 GHz is limited at 20 dBm (in Europe). Alternatively, if the assumed minimal separation from an AP decreases (for a fixed value of $E_{\max}^{ds}$), the maximally allowed EIRP decreases and more APs are

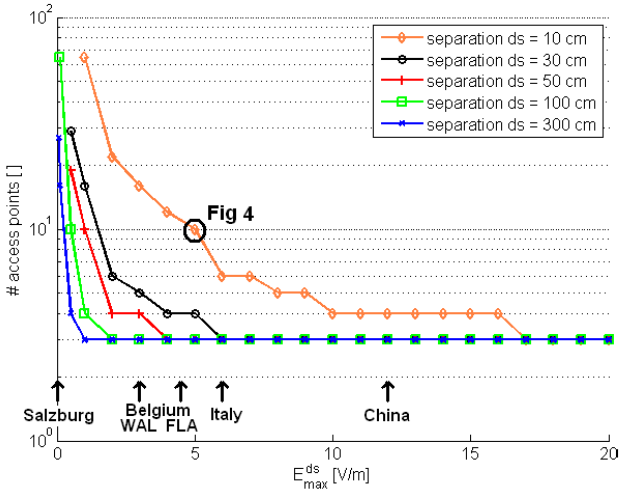

Figure 5. Number of APs needed to provide the required coverage on the building floor, as a function of the maximal limit $E_{\max}$ for different minimal separations from the AP, and indication of limits or recommendations in different regions (WAL = Wallonia, FLA = Flanders; both are Belgian regions).

needed to cover the building floor. E.g., for Flanders, the number of required access points increases from 3 to 11 if the assumed minimal separation from the access point decreases from 1 m to 10 cm.

As an example of the exposure limitation (and calculation) algorithm, Fig. 4 shows the resulting exposure map for the proposed configuration for a maximal electric field $E_{ds}^{\max}$ of 5 V/m at a separation d_s of 10 cm from the AP. This is indicated as one point ('Fig. 4') in Fig. 5. This means that it is assumed that the EIRP of the access points will be chosen in such a way that, as long as the human does not approach the access point closer than 10 cm (= separation d_s), the experienced field strength will not exceed 5 V/m (= $E_{ds}^{\max}$). For this example configuration, 10 access points (with an EIRP of 9 dBm) are needed. The electric-field strength for this configuration is visualized in Fig. 4 using a colour code. The APs are not indicated in the figure, but it is clear that their locations correspond to the center of the lighter zones where the exposure is the highest. Obviously, the electric-field strength decreases when moving away from the APs. The optimized low-exposure network for the ground plan of Fig. 4 corresponds with $E_{\max}^{10\,\mathrm{cm}} = 5\,\mathrm{V/m}$ and is also indicated in Fig. 5.

Table 2 shows the number of APs needed to cover the building floor depicted in Fig. 4 (see Section 5.1) for an assumption of a maximal EIRP of 20 dBm, for different AP-to-human separations and for some specific exposure limits (or recommendations) in different countries. The different exposure limits cause large differences in the required number of APs (and their maximal EIRP): for a separation d_s of 10 cm, the number of required access points varies from 3 (ICNIRP) to 16 (Wallonia). It is clear that for very restrictive limits (low $E_{\max}$ values), network planning becomes extremely difficult (e.g., Salzburg, where more than 75 access points would be needed if this guideline had to be followed). When the assumed 'separations' increase, the number of required access points decreases of course.

6. APPLICATION OF EXPOSURE MINIMIZATION ALGORITHM

Three scenarios will be considered for the exposure minimization. In a first scenario, we will illustrate the four optimization phases (see Section 4.2) for a *homogeneous* WiFi network with a throughput of 54 Mbps for one user in the service area of each access point. In a second scenario, the influence of the required throughput on the obtained field strength distribution will be assessed for *homogeneous* WiFi networks. Finally, in the third scenario, a *heterogeneous* WiFi-LTE network will be optimized with respect to exposure.

6.1. Configuration and Scenarios

Human exposure will be minimized for the same office building as before (see Fig. 4). Three different scenarios will be investigated for this building floor. However, the scenarios have in common that coverage will have to be provided throughout the entire building, except in the shaded rooms (see Section 4.2.1). Access points are always placed at a height of 200 cm above ground level and the receiver is assumed at a height of 100 cm above ground level. The minimization is performed using the metric E_M (see Section 4.2.1): the configuration yielding the lowest possible average of E_{50} and E_{95} is targeted and locations within a horizontal distance of 30 cm from the transmitters are left out of the electric-field strength distribution calculation. The three investigated scenarios are the following.

(1) In the first (homogeneous) scenario, only WiFi access points are placed over the entire building floor in order to provide coverage for HD video streaming (54 Mbps), based on the specifications

of a WiFi 802.11 g reference receiver (see Table 1). The four optimization phases defined in Section 4.2 will be discussed.

(2) In the second (homogeneous) scenario, a similar approach as in the first scenario is followed. However, we will now assess the influence of the required throughput (varying from 6 to 54 Mbps) on the number of required access points and the distribution of the electric-field strength. Also, the exposure improvement when switching from a traditional network deployment (with high-power transmitters) to an exposure-optimized network deployment is investigated. With 'traditional' network design, we mean a design that provides network coverage with as few access points as possible. Obviously, the access points will then transmit at the maximally allowed power. Coverage calculations are again based on the specifications of the WiFi 802.11g reference receiver (see Table 1).

(3) In the third (heterogeneous) scenario, *one* LTE femtocell at 2600 MHz is present in the building, with an EIRP of 10 dBm, a bandwidth of 20 MHz and a 3 : 1 downlink-uplink ratio. Previous research has indicated that femtocell downlink traffic may cause significant exposure values. In this scenario, the femtocell EIRP cannot be decreased and is assumed to be fixed at 10 dBm. The femtocell has a fixed location and WiFi access points are added to provide a coverage of 18 Mbps (vs. 54 Mbps in scenario 1). We choose a lower throughput (18 Mbps) than in scenario 1 (54 Mbps), because usually, lower throughputs will be expected from LTE femtocells. For the heterogeneous scenario, we assume a 4G receiver (WiFi and LTE) that is able to automatically switch to the transmitter (access point or femtocell) that provides it with the best coverage. The four optimization phases defined in Section 4.2 will be discussed.

In the following, these three scenarios will be elaborated on.

6.2. Scenario 1: Exposure Minimization Phases for a Homogeneous WiFi Network (54 Mbps)

In this section, the four exposure minimization phases described in Section 4.2 will be applied to a homogeneous WiFi network (see Section 4.1) for a required throughput of 54 Mbps. Table 3 lists the results of each of the phases.

In phase 1, the WHIPP optimization module places access points on the ground plan, with the empty ground plan of the considered building floor as an input to the algorithm. 23 Access points with an EIRP of 1 dBm are needed, yielding a median electric-field strength

E_{50} of 0.053 V/m and a 95%-percentile value E_{95} of 0.190 V/m. E_M equals 0.122 V/m. Fig. 6 shows the result of phase 1 for the considered building floor after this first optimization phase, i.e., optimal network design with only WiFi access points with an EIRP of 1 dBm.

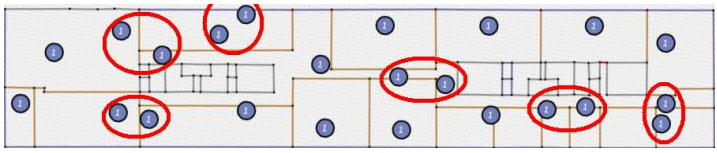

Figure 6. Network layout after first exposure minimization phase. (AP = dot, EIRP is indicated within dot, circles around APs indicate mergeable access point pairs).

In phase 2, access point pairs are merged (see Fig. 3, phase 2). The six access point pairs that are circled in Fig. 6, can be merged with a resulting lower global exposure E_M (see Section 4.2.1). Fig. 7 shows the resulting network after the second optimization phase (phase 2). The newly placed access points are circled in Fig. 7 and have EIRPs between 0 and 3 dBm. Although coverage is now provided with a lower number of access points (17 (with EIRP between 1 and 3 dBm) instead of 23 (with EIRP of 1 dBm)), the E_{50} and E_{95} values also decrease, to respective values of 0.049 V/m and 0.174 V/m. E_M decreases from 0.122 V/m to 0.112 V/m.

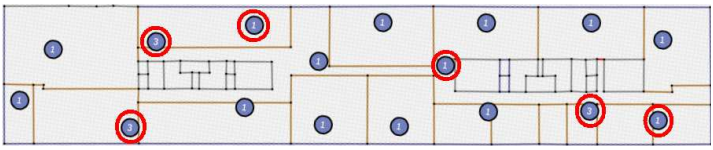

Figure 7. Network layout after merging access point pairs (second exposure minimization phase) (AP = dot, EIRP is indicated within dot, circles around APs indicate newly placed access points in phase 2).

In a third phase, it is investigated if access points can be removed by increasing the transmit power of the surrounding access points in an optimal way. This would for example be the case if there is one access point that is more or less circularly surrounded by other access points that are within a reasonable distance from the center transmitter. Removing the center access point while increasing each (or some) of the powers of the surrounding access points with a few dB could then 'fill' the coverage gap that arose in the center by removing the (center) access point. For the building floor under test however, no access

points could be removed, due to the 'homogeneous' distribution of the access points over the building floor. By a homogeneous distribution, we mean that each of the access points covers a substantial and more or less equal part of the coverage area.

In the final phase 4, transmit powers are lowered where possible. For the investigated building floor, it is possible to lower the EIRP of six access points without losing the requested coverage. The requested throughput is still achieved when we decrease the EIRP of the access points circled in Fig. 8, from 1 dBm in Fig. 7 to 0 dBm in Fig. 8. Final E_{50} and E_{95} values are 0.048 V/m and 0.169 V/m, E_M decreases further to 0.108 V/m.

Traditionally, network designers try to provide coverage with the least amount of access points possible. In the considered building and for a traditional network deployment (see Section 4.1, scenario 2), a network with (three) access points with an EIRP of 20 dBm is designed. The exposure values for a 'traditional' network design of the investigated building are compared with the four exposure optimization phases in Table 3. Compared to the traditional deployment, the final exposure-optimized network (after phase 4) has an E_M value that is reduced by more than a factor 3. Also, the standard deviation σ of

Table 3. Number of access points (#APs), their EIRP needed to cover the building floor of Fig. 4, the resulting median (E_{50}) and 95%-percentile (E_{95}) exposure values, the standard deviation σ of the field values, the E_M value, and the gain $\frac{E_M}{E_M^{\text{traditional}}}$ with respect to a traditional network deployment for the different optimization cases for a homogeneous network providing a throughput of 54 Mbps.

Case	**#APs** [-]	EIRP **[dBm]**	$\mathbf{E_{50}}$ **[V/m]**	$\mathbf{E_{95}}$ **[V/m]**	σ **[V/m]**	$\mathbf{E_M}$ **[V/m]**	$\frac{\mathbf{E_M}}{\mathbf{E_M^{traditional}}}$ [-]
Homogeneous WiFi network (54 Mbps)							
After phase 1	23	1	0.053	0.190	0.071	0.122	2.70
After phase 2	17	between 1 and 3	0.049	0.174	0.069	0.112	2.94
After phase 3	17	between 1 and 3	0.049	0.174	0.069	0.112	2.94
After phase 4	17	between 0 and 3	0.048	0.169	0.067	0.108	3.05
Traditional	3	20	0.114	0.544	0.194	0.329	1

the electric-field strengths on the building floor is noticeably higher for the traditional deployment. The exposure-optimized network causes a more homogeneous field strength distribution.

Figure 9 shows the cumulative distribution function of the electric-field values on the building floor of Fig. 4 for the different optimization phases and for a traditional network deployment. Fig. 9 and Table 3 show that the largest gain is obtained by using low-power transmitters in the first optimization phase ('Phase 1' vs. 'Traditional'). According to our metric E_M, the first optimization phase yields a gain of a factor 2.70. The next optimization phases add another gain up to a factor 2.94, while at the same time reducing the number of access points from 23 to 17. The steeper slope of the exposure-optimized cdfs in Fig. 9, indicate the lower standard deviation and thus the more homogeneous distribution of the field strengths compared to a traditional network design.

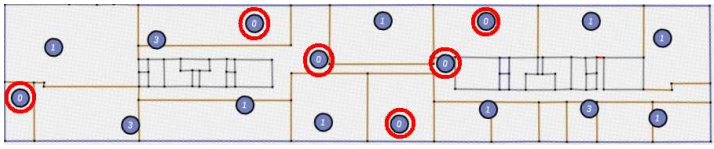

Figure 8. Network layout after final exposure minimization phase (AP = dot, EIRP is indicated within dot, circles around APs indicated access point for which EIRP has been lowered compared to phase 3).

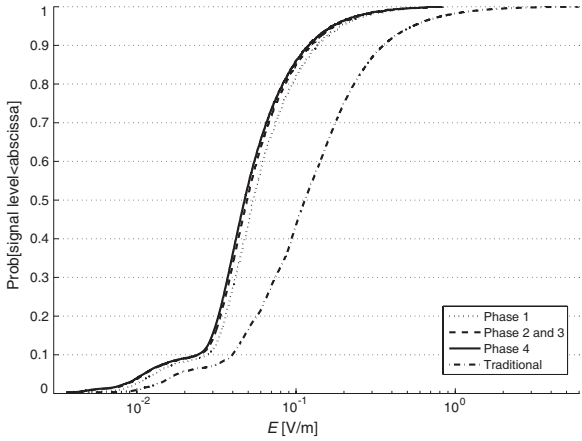

Figure 9. Cumulative distribution function of electric-field values on the building floor of Fig. 4 for the different optimization phases and for a traditional network deployment.

It should be noted though, that in real-life network deployments, the total installation and operational cost will often be an important factor in the design of the network. Seventeen access points are required for our exposure-optimized network, almost six times more than for the traditional design. The exposure-optimized network not only has a higher cost, but also a higher energy consumption. A planned extension of the network planner will enable a trade-off between cost, energy consumption, and exposure.

6.3. Scenario 2: Comparison of Traditional vs. Exposure-optimized Deployment for Different Throughputs in a Homogeneous WiFi Network

In the previous section, a homogeneous WiFi network providing a throughput of 54 Mbps is investigated. However, it is expected that the required throughput on the building floor will have a huge influence on the field strength distribution. In this section, we will, therefore, assess the influence of the throughput requirement on the electric-field strength distribution and the network design and we will make a comparison of a traditional network design and an exposure-optimized network design.

Table 4 summarizes the number of access points (#APs) and their EIRP needed to cover the building floor of Fig. 4 and the field strength distribution parameters (median (E_{50}), 95%-percentile (E_{95}), E_M, and standard deviation σ) for a traditional network deployment (EIRP of APs = 20 dBm) and the exposure-optimized deployment (according to the algorithm of Section 4.2, after phase 4). Table 4 shows that for lower throughputs, the building floor can be covered with a substantially lower number of access points. E.g., the exposure-optimized network requires 17 access points for a throughput of 54 Mbps, while for a throughput of 6 Mbps, only two access points are needed. The table shows that the exposure-optimized network reduces the value of the metric E_M by a factor 3.05 for a throughput of 54 Mbps, up to a factor 5.87 for a low throughput (6 Mbps) (column 'gain optimized vs. traditional deployment').

Figure 10 shows the cumulative distribution functions of the electric-field values on the building floor of Fig. 4 for different throughputs for the traditional network deployment vs. the exposure-optimized network. Fig. 10 and Table 4 show that for lower throughputs, also the field strength values decrease, as expected. The median (E_{50}) and 95%-percentile (E_{95}) drop, from 0.048 V/m and 0.169 V/m respectively, to 0.007 V/m and 0.050 V/m respectively. Of course, for all investigated throughputs, the exposure-optimized networks cause noticeably lower field strengths on the building floor.

Fig. 10 and Table 4 show that the exposure-optimized network for 54 Mbps has a similar median (E_{50}) value as the traditional deployment for 36 Mbps (0.048 V/m vs. 0.045 V/m respectively). However, the exposure-optimized network has a more homogeneous field distribution (steeper slope of the cdf for optimal design in Fig. 10, lower E_{95} and σ in Table 4). An increased field strength homogeneity (low variance) on the building floor has also been taken into account in the optimization metric of [21].

Table 4. Number of access points (#APs) and their EIRP needed to cover the building floor of Fig. 4 and resulting median (E_{50}), 95%-percentile (E_{95}), and global (E_M) exposure values, standard deviations σ, $\frac{E_{\mathrm{ICNIRP}}}{E_M}$ ratio for different intended throughputs for a traditional network deployment vs. an exposure-optimized network deployment, and gain $\frac{E_M}{E_M^{\mathrm{traditional}}}$ of the exposure-optimized network with respect to the traditional network deployment.

Throughput [Mbps]	Conguration	#APs [-]	EIRP [dBm]	E_{50} [V/m]	E_{95} [V/m]	σ [V/m]	E_M [V/m]	$\frac{E_{\mathrm{ICNIRP}}}{E_M}$ [-]	$\frac{E_M}{E_M^{\mathrm{traditional}}}$ [-]
54	traditonal	3	20	0.114	0.544	0.194	0.329	185	3.05
	optimized	17	between 0 and 3	0.048	0.169	0.067	0.108	565	
36	traditonal	2	20	0.045	0.386	0.144	0.236	258	3.63
	optimized	7	between −1 and 4	0.025	0.102	0.035	0.065	938	
24	traditonal	1	20	0.034	0.277	0.102	0.176	347	3.74
	optimized	5	between −2 and 1	0.017	0.075	0.026	0.047	1298	
18	traditonal	1	20	0.034	0.277	0.102	0.176	347	4.09
	optimized	4	−1 or 0 or 1	0.013	0.073	0.026	0.043	1419	
12	traditonal	1	20	0.034	0.277	0.102	0.176	347	4.51
	optimized	3	−4 or 1 or 1	0.011	0.062	0.022	0.039	1564	
6	traditonal	1	20	0.034	0.277	0.102	0.176	347	5.87
	optimized	2	−1 and 2	0.007	0.050	0.018	0.030	2033	

The gain G_E^i (in absolute values) of using an exposure-optimized network instead of a traditional deployment is defined as the difference of a certain percentile value i for the two cases. In this paper, i will be either 5, 10, 25, 50, 75, 90, or 95, but of course any percentile value can be considered.

$$G_E^i = E_{\mathrm{trad}}^i - E_{\mathrm{opt}}^i \ [\mathrm{V/m}], \tag{8}$$

with E_{trad}^i the i-th percentile of the electric-field values on the building floor for a traditional network deployment, and E_{opt}^i the i-th percentile

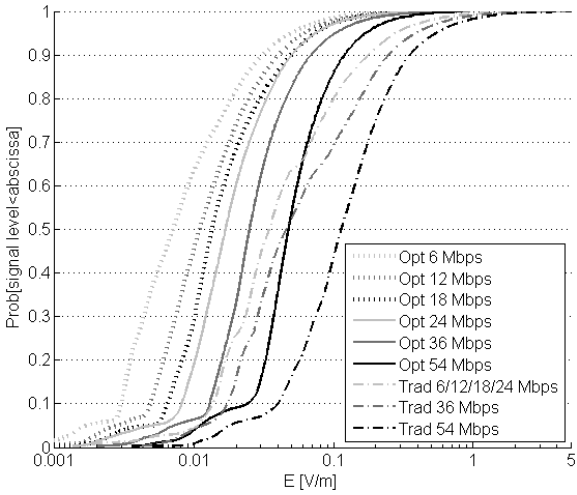

Figure 10. Cumulative distribution function of electric-field values on the building floor of Fig. 4 for different throughputs for the traditional network deployment vs. the exposure-optimized network (Opt = exposure-optimized network, Trad = traditional network design).

of the electric-field values on that building floor for an exposure-optimized design. A value of G_E^i greater than zero thus means that the exposure-optimized network has better exposure characteristics than the traditional deployment.

Figure 11 shows the gains G_E^i when using an exposure-optimized network instead of a traditional deployment for different required throughputs. The figure shows that G_E^i increases for higher throughputs (54 Mbps vs. 36 Mbps and 36 Mbps vs. 24 Mbps). This means that for higher throughputs, exposure optimization is more beneficial (in absolute values). However, for increasing throughputs below 24 Mbps (i.e., from 6 Mbps to 18 Mbps), the gain decreases. This is due to the network planning for traditional deployments: for throughputs of 24 Mbps and lower, 1 access point with an EIRP of 20 dBm suffices to cover the whole building floor, yielding equal exposure characteristics, irrespective of the throughput (see Table 4, traditional, throughput $\leq$ 24 Mbps). Since in the exposure-optimized case, the network planner is able to decrease the total exposure for decreasing throughputs ($\leq$ 24 Mbps), the gain increases for decreasing throughputs $\leq$ 24 Mbps.

Figure 11 also shows that for higher percentiles, the gain G_E^i increases, e.g., $G_E^{95} = 0.375\,\mathrm{V/m}$ vs. $G_E^{50} = 0.066\,\mathrm{V/m}$ for a

throughput of 54 Mbps. This means that in exposure-optimized networks, especially the high field values are lowered by the proposed new design method, leading to a more homogeneous field distribution. This was already shown by the lower standard deviation in Table 4 and the steeper slope of the cdfs for optimal exposure design in Fig. 10 compared to the traditional deployment (more homogeneous distribution).

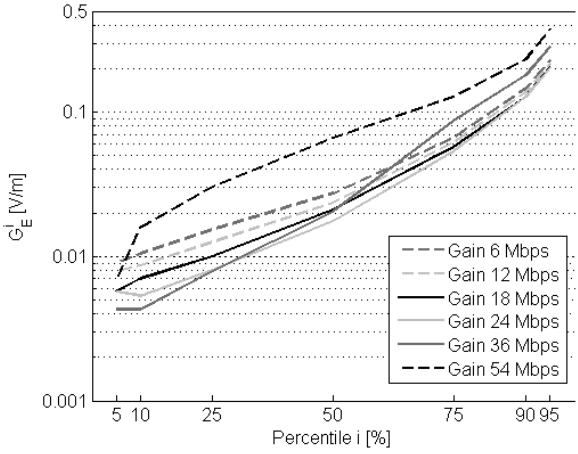

Figure 11. Gain in electric-field strength as a function of the percentile of the electric-field strengths on the building floor of Fig. 4 for different required throughputs.

The exposure optimization algorithm allows the network planner to quickly assess the number of required access points and their power, and the coverage and exposure characteristics of the resulting network.

6.4. Scenario 3: Exposure Minimization Phases for a Heterogeneous Network WiFi-LTE Network (18 Mbps)

In this section, the four exposure minimization phases described in Section 4.2 will be applied to a *heterogeneous* (WiFi and LTE) network (see Section 4.1). In the heterogeneous scenario, one LTE femtocell operating at 2.6 GHz with a fixed transmit power and location is present as shown in Fig. 12 (top right of building plan). The femtocell is indicated with a hexagon with the EIRP value inside. During the successive optimization phases, the femtocell settings are fixed, only the WiFi APs are assumed to be adaptable. Since the requested coverage (18 Mbps) cannot be provided by only the femtocell, WiFi

access points will have to be added according to the algorithm discussed in Section 4.2 (see also Fig. 3).

In the first optimization phase, three WiFi access points with an EIRP of 1 dBm are added (see Fig. 12) to provide the necessary coverage on the building floor. This number of access points is substantially lower than for the homogeneous scenario. This is mostly due to the lower throughput requirement (18 Mbps vs. 54 Mbps), but also partly due to the coverage of the femtocell. For this network, E_{50} equals 0.021 V/m, E_{95} equals 0.135 V/m, and E_M equals 0.079 V/m. Due to the small number of WiFi access points (three) and their optimal placement after optimization phase 1, no further optimizations are possible in phase 2 or phase 3. In phase 4, the EIRP of two of the three WiFi access points (circled in Fig. 12) can be lowered to 0 dBm, resulting in final E_{50}- and E_{95}-values of 0.020 V/m and 0.135 V/m respectively. E_M only slightly decreases to 0.077 V/m. A gain of a factor 2.39 is obtained, compared to a traditional network deployment.

Comparison of the exposure values of Tables 5 and 3 (heterogeneous vs. homogeneous) show that electric-field values are lower for the heterogeneous network than for the homogeneous network. Although a femtocell with a relatively high EIRP of 10 dBm is present, the lower exposure values are due to the lower throughput requirement for the heterogeneous case (18 Mbps vs. 54 Mbps). Table 4 (homogenenous 18 Mbps) indeed shows that for a throughput of 18 Mbps, the optimized homogeneous network (with 4 WiFi access points) produces lower field values and a lower variance than the optimized heterogeneous network (Table 5), due to the relatively high transmit power of the femtocell (10 dBm), compared to the transmit powers of the WiFi access points (between −1 and 1 dBm, see Table 4). The heterogeneous network has an E_M value of 0.077 V/m and a standard deviation of 0.066 V/m, compared to an E_M value of 0.043 V/m and a standard deviation of 0.026 V/m for the homogeneous case.

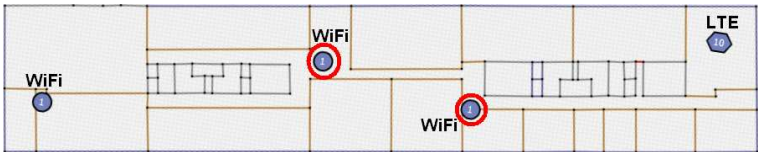

Figure 12. Network layout after third exposure minimization phase (WiFi AP = dot, LTE femtocell = hexagon, EIRP is indicated within dot or hexagon, circles around APs indicate access points for which EIRP is lowered to 0 dBm in phase 4).

Table 5. Number of access points (#APs), their EIRP needed to cover the building floor of Fig. 4, the resulting median (E_{50}) and 95%-percentile (E_{95}) exposure values, the standard deviation σ of the field values, the E_M value, and the gain $\frac{E_M}{E_M^{\text{traditional}}}$ with respect to a traditional network deployment for the different optimization cases for a heterogeneous network providing a throughput of 18 Mbps.

Case	**#APs** [-]	EIRP [**dBm**]	$\mathbf{E_{50}}$ [**V/m**]	$\mathbf{E_{95}}$ [**V/m**]	σ [**V/m**]	$\mathbf{E_M}$ [**V/m**]	$\frac{\mathbf{E_M}}{\mathbf{E_M^{traditional}}}$ [-]
Heterogeneous LTE-WiFi network (18 Mbps)							
After phase 1	1 LTE 3 WiFi	10 (femto) 1 (WiFi)	0.021	0.135	0.068	0.079	2.33
After phase 2	1 LTE 3 WiFi	10 (femto) 1 (WiFi)	0.021	0.135	0.068	0.079	2.33
After phase 3	1 LTE 3 WiFi	10 (femto) 1 (WiFi)	0.021	0.135	0.068	0.079	2.33
After phase 4	1 LTE 3 WiFi	10 (femto) 0 or 1 (WiFi)	0.020	0.135	0.066	0.077	2.39
Traditional	1 LTE 1 WiFi	10 (femto) 20 (WiFi)	0.051	0.316	0.184	0.184	1

7. VALIDATION OF DOMINANT TRANSMITTER ASSUMPTION

In Section 3.3, it was stated that for the exposure calculations, only the dominant transmitter has been taken into account. This assumption will now be validated for two different topologies: a dense network with low-power transmitters and a traditional network deployment. The investigated dense network is the homogeneous WiFi network depicted in Fig. 8, the traditional network is a network that provides the same coverage, but with only 3 access points with a high transmit power (EIRP of 20 dBm). Two calculation methods will be applied for the field strengths E at each building floor location. The first calculation method calculates E as E_{dom}, the method that has been used throughout this paper: at each location, only the contribution of the dominant transmitter (the transmitter providing the receiver with the highest incident field) is considered. The second calculation method calculates E as E_{total} (see Section 3.3): at each location, the fields from all sources are considered, according to Equation (4).

Table 6 shows the value of E_M for these two network topologies

for two calculation methods for the total electric field. The table shows that the simplification of only taking into account the dominant transmitter ($E = E_{\text{dom}}$) causes limited errors of at most 5.45% for a very dense network and less than 1% for a traditional network deployment. Importantly, using E_{dom} instead of E_{total} leads to calculations that are up to 200 times faster.

Table 6. Comparison of E_M and E_{99} values for a traditional and an optimized network deployment for the two calculation methods.

Topology	$\mathbf{E_M}$			$\mathbf{E_{99}}$		
	$\mathbf{E_{dom}}$ [V/m]	$\mathbf{E_{total}}$ [V/m]	error	$\mathbf{E_{dom}}$ [V/m]	$\mathbf{E_{total}}$ [V/m]	error
Traditional	0.329	0.332	0.90%	1.345	1.345	0.03%
Optimized	0.108	0.114	5.45%	0.360	0.362	0.44%

As a validation of the exposure limitation algorithm, where it is required that a certain field strength level is not exceeded, the 99%-percentile value E_{99} of all recorded field values is investigated for the two calculation methods. Table 6 shows that the use of E_{dom} instead of E_{total} has no influence (error less than 0.5%) on the observed highest field strengths on the building floor, for either of the two topologies (errors of less than a half percent).

8. CONCLUSIONS AND FUTURE WORK

A heuristic indoor network planner for exposure calculation and optimization in wireless homogeneous and heterogeneous networks is developed, with which networks are automatically jointly optimized for both coverage and electromagnetic exposure. The implemented exposure models are validated by simulations and measurements. As a first feature, an algorithm for exposure limitation is presented and applied to a WiFi network in an office building, which is optimized in order not to exceed a user-defined maximal electric-field strength at a certain separation from the APs. It is shown that higher allowed exposure limits and higher separations between the AP and the human, allow higher transmit powers and hence, a lower number of APs is required to provide coverage. The required number of access points greatly differs for different countries in the world, because of different exposure limits. As a second feature, an exposure minimization algorithm is presented and applied to a wireless homogeneous WiFi and a heterogeneous WiFi-LTE network, using a new metric that is

simple but accurate. Depending on the required throughput, field strength reductions of a factor 3 to 6 and a higher homogeneity of the field strength distribution on the building floor are obtained, compared to traditional network deployments. It is shown that exposure minimization is more beneficial for high than for low throughput requirements and that high field values are more reduced than low field values. Finally, it is shown that only taking into account the dominant transmitter for exposure calculations leads to only very limited prediction errors.

Future research may investigate more complex metrics, where different locations in the optimized building have different weights, depending on the expected distribution of the human presence at the different locations. Also, the influence of the access point duty cycle on the exposure can be investigated [30], as well as exposure due to uplink traffic. Finally, an algorithm for a joint optimization of human exposure, total (deployment and operational) cost, and energy consumption will be developed.

ACKNOWLEDGMENT

This work was supported by the IWT-SBO SymbioNets project. W. Joseph is a Post-Doctoral Fellow of the FWO-V (Research Foundation-Flanders).

REFERENCES

1. Ji, Z., B.-H. Li, H.-X. Wang, H.-Y. Chen, and T. K. Sarkar, "Efficient ray-tracing methods for propagation prediction for indoor wireless communications," *IEEE Antennas and Propagation Magazine*, Vol. 43, No. 2, 41–49, April 2001.
2. Torres, R., L. Valle, M. Domingo, and M. Diez, "CINDOOR: an engineering tool for planning and design of wireless systems in enclosed spaces," *IEEE Antennas and Propagation Magazine*, Vol. 41, No. 4, 11–22, September 1999.
3. Wlfle, G., R. Wahl, P. Wertz, P. Wildbolz, and F. Landstorfer, "Dominant path prediction model for indoor scenarios," *German Microwave Conference*, Ulm, Germany, April 2005.
4. Dimitriou, A. G., S. Siachalou, A. Bletsas and J. N. Sahalos, "An efficient propagation model for automatic planning of indoor wireless networks," *3rd European Conference on Antennas and Propagation*, Barcelona, Spain, April 12–16, 2010.
5. Sebastiao, P., R. Tome, F. Velez, A. Grilo, F. Cercas, D. Robalo,

A. Rodrigues, F. F. Varela, and C. X. P. Nunes, "WLAN planning tool: A techno-economic perspective," *COST 2100 TD(09)935 Meeting*, Vienna, Austria, September 28–30, 2009.

6. Phaiboon, S., "An empirically based path loss model for indoor wireless channels in laboratory building," *IEEE Region 10 Conference on Computers, Communications, Control and Power Engineering*, Vol. 2, 1020–1023, October 2002.
7. Keenan, J. M. and A. J. Motley, "Radio coverage in buildings," *BTSJ*, Vol. 8, No. 1, 19–24, January 1990.
8. Plets, D., W. Joseph, K. Vanhecke, E. Tanghe, and L. Martens, "Coverage prediction and optimization algorithms for indoor environments," *EURASIP Journal on Wireless Communications and Networking, Special Issue on Radio Propagation, Channel Modeling, and Wireless, Channel Simulation Tools for Heterogeneous Networking Evaluation*, Vol. 1, 2012, http://jwcn.eurasipjournals.com/content/2012/1/123.
9. Plets, D., W. Joseph, E. D. Poorter, L. Martens, and I. Moerman, "Concept and framework of a self-regulating symbiotic network," *EURASIP Journal on Wireless Communications and Networking*, Vol. 2012, No. 340, 2012, http://jwcn.eurasipjournals.com/content/2012/1/340.
10. Deruyck, M., E. Tanghe, W. Joseph, and L. Martens, "Modelling and optimization of power consumption in wireless access networks," *Elsevier Computer Communications (Special Issue: European Wireless 2010)*, Vol. 34, No. 17, 2036–2046, November 2011.
11. Joseph, W., L. Verloock, F. Goeminne, G. Vermeeren, and L. Martens, "Assessment of RF exposures from emerging wireless communication technologies in different environments," *Health Physics*, Vol. 102, No. 2, 161–172, February 2012.
12. IEEE Std C95.1, "IEEE standard for safety levels with respect to human exposure to radio frequency electromagnetic fields, 3 kHz to 300 GHz," 1999.
13. ICNIRP, "Guidelines for limiting exposure to time-varying electric, magnetic, and electromagnetic fields (up to 300 GHz)," *Health Physics*, Vol. 74, No. 4, 494–522, April 1998.
14. Deruyck, M., W. Vereecken, W. Joseph, B. Lannoo, M. Pickavet, and L. Martens, "Reducing the power consumption in wireless access networks: Overview and recommendations," *Progress In Electromagnetics Research*, Vol. 132, 255–274, 2012.
15. Foster, K. R., "Radiofrequency exposure from wireless LANs using Wi-Fi technology," *Health Physics*, Vol. 92, 280–289, 2007.

16. Joseph, W., P. Frei, M. Roösli, G. Thuróczy, P. Gajsek, T. Trcek, J. Bolte, G. Vermeeren, E. Mohler, P. Juhsz, V. Finta, and L. Martens, "Comparison of personal radio frequency electromagnetic field exposure in different urban areas across Europe," *Environmental Research*, Vol. 110, No. 7, 658–663, 2010.
17. Joseph, W., P. Frei, M. Roösli, G. Vermeeren, J. Bolte, G. Thuróczy, P. Gajsek, T. Trcek, E. Mohler, P. Juhasz, V. Finta, and L. Martens, "Between-country comparison of whole-body SAR from personal exposure data in urban areas," *Bioelectromagnetics*, Vol. 33, No. 8, 682–694, December 2012.
18. Frei, P., E. Mohler, A. Bürgi, J. Fröhlich, G. Neubauer, C. Braun-Fahrländer, and M. Roosli, "A prediction model for personal radio frequency electromagnetic field exposure," *Science of The Total Environment*, Vol. 408, No. 1, 102–108, 2009.
19. Boursianis, A., P. Vanias, and T. Samaras, "Measurements for assessing the exposure from 3G femtocells," *Radiation Protection Dosimetry*, Vol. 150, No. 2, 158–167, 2012.
20. Perentos, N., S. Iskra, A. Faraone, R. McKenzie, G. Bit-Babik, and V. Anderson, "Exposure compliance methodologies for multiple input multiple output (MIMO) enabled networks and terminals," *IEEE Transactions on Antennas and Propagation*, Vol. 60, 644–653, 2012.
21. Russo, P., G. Cerri, and V. Vespasiani, "A numerical coefficient for evaluation of the environmental impact of electromagnetic fields radiated by base stations for mobile communications," *Bioelectromagnetics*, Vol. 31, 613–621, 2010.
22. Cerri, G., R. De Leo, D. Micheli, and P. Russo, "Base-station network planning including environmental impact control," *IEE Proceedings — Communications*, Vol. 151, No. 3, 197–203, June 2004.
23. Koutitas, G., "Green network planning of single frequency networks," *IEEE Transactions on Broadcasting*, Vol. 56, No. 4, 541–550, December 2010.
24. Deruyck, M., W. Joseph, and L. Martens, "Power consumption model for macrocell and microcell base stations," *Transactions on Emerging Telecommunication Technologies*, 2012, doi:10.1002/ett.2565.
25. ITU-R Recommendation P.1546, "Method for point-to-area predictions for terrestrial services in the frequency range 30 MHz to 3000 MHz," 2003–2005.
26. Verloock, L., W. Joseph, G. Vermeeren, and L. Martens, "Procedure for assessment of general public exposure from wlan

in offices and in wireless sensor network testbed," *Health Physics*, Vol. 98, No. 4, 628–638, 2012.

27. European Telecommunications Standards Institute, ETSI EN 300 328-2 v1.5.1, "Electromagnetic compatibility and Radio spectrum Matters (ERM); Wideband Transmission systems; Data transmission equipment operating in the 2.4 GHz ISM band and using spread spectrum modulation techniques; Part 2: Harmonized EN covering essential requirements under article 3.2 of the R&TTE Directive Edition: 1.2.1," August 2004.
28. Plets, D., W. Joseph, K. Vanhecke, E. Tanghe, and L. Martens, "Simple indoor path loss prediction algorithm and validation in living lab setting," *Wireless Personal Communications*, 1–18, 10.1007/s11277-011-0467-4, 2013, http://dx.doi.org/10.1007/s11277-011-0467-4.
29. International Commission on Non-ionizing Radiation Protection (ICNIRP), "Guidelines for limiting exposure to time-varying electric, magnetic, and electromagnetic fields (up to 300 GHz)," *Health Physics*, Vol. 74, No. 4, 494–522, April 1998.
30. Joseph, W., D. Pareit, G. Vermeeren, D. Naudts, L. Verloock, L. Martens, and I. Moerman, "Determination of the duty cycle of WLAN for realistic radio frequency electromagnetic field exposure assessment," *Progress in Biophysics & Molecular Biology*, October 2012.